

Magnetic-field dependence of the ac susceptibility in granular $\text{YBa}_2\text{Cu}_3\text{O}_7$: Data and models

Youngtae Kim,* Q. Harry Lam, and C. D. Jeffries

Physics Department, University of California, Berkeley, California 94720

and Materials and Chemical Sciences Division, Lawrence Berkeley Laboratory, Berkeley, California 94720

(Received 1 August 1990)

For a sintered rod of $\text{YBa}_2\text{Cu}_3\text{O}_7$ at 78.3 K, detailed data are reported for the complicated dependence of the ac susceptibility $\tilde{\chi} = \chi' - i\chi''$ on applied ac and dc fields, ascribed to the inter- and intragranular components of the material. The intergranular data are understood in detail by a modified critical-state model, assuming a critical current density $J_c(H) \sim H^{-2}$. $\tilde{\chi}(H_{dc})$ also displays hysteresis which is not readily explicable by this model.

Owing to its granular nature the superconductor $\text{YBa}_2\text{Cu}_3\text{O}_7$ displays an ac susceptibility $\tilde{\chi} = \chi' - i\chi''$ with elaborate dependence on temperature T and ac and dc applied fields H_a .¹ Bulk specimens are generally assumed to consist of superconducting grains connected by weak links, referred to as intra- and intergranular components, respectively; both contribute to $\tilde{\chi}$ at high and low fields, respectively. A semiquantitative interpretation of the data, particularly the temperature dependence, has been obtained by calculations^{2,3} based on critical-state models.⁴⁻⁶ The key to a more detailed understanding of $\tilde{\chi}(H_a)$ in the low-field region, our concern in this report, is the dependence of the critical current density J_c on field. We present detailed data as well as a modified critical-state model, finding very good agreement.^{7,8} The model also predicts well the observed harmonic generation.⁹

Experimental results. The data were obtained for a cylinder (radius $R = 0.85$ mm, length = 10.5 mm) fabricated from sintered polycrystalline $\text{YBa}_2\text{Cu}_3\text{O}_7$.¹⁰ This was encased in a thin-wall quartz tube wound with a 380-turn coil and connected to a digital impedance analyzer (HP 4192A), which provided a controlled ac current and thus an ac field $H_1 \cos(2\pi ft)$ on the sample. The analyzer also measured the effective inductance L and resistance R of the coil. The sample was also subject to a quasi-dc field H_{dc} from a coaxial copper solenoid driven by a symmetric-triangle ramp current at $f_{\text{scan}} \approx 0.0025$ Hz from a synthesizer (HP 3325A). All instruments and data acquisition were computer controlled. For a given set of controlled parameters (T, H_{dc}, H_1, f) , three were held constant and the other one was varied over its range, both with and without the sample in the coil; the data sets were subtracted to give ΔL and ΔR , from which χ' and χ'' were computed, including small corrections for demagnetization factor and coil resonance.⁸ All the data shown, except for Fig. 2(h), were taken with the same sample at $T = 78.3$ K and $f = 10$ kHz. Figure 1(a) shows the dispersive component of the susceptibility, χ' vs H_{dc} , for selected values of H_1 : 0.03–7.91 Oe; these data were taken by cooling the sample in zero field and slowly ramping H_{dc} from 0 to 40 Oe, down to 0, down to -40 Oe, etc. Our model predictions, in Fig. 1(b), are seen to

be in unusually good and detailed agreement with the data. Similarly, the data, Fig. 1(f), for the absorption component, χ'' vs H_{dc} , are well predicted by the model, Fig. 1(g), except for a small hysteresis between increasing and decreasing fields scans. For frequencies in the range $10^3 < f < 10^6$ Hz both χ' and χ'' show a very small dependence ($< 1\%$) on f , implying that the loss mechanism is hysteresis, predicted by the critical-state model. Data for $\chi'(H_1)$ are shown in Fig. 2(a) for selected values of H_{dc} from 0 to 15 Oe; these are also well predicted by the model, Fig. 2(b). Data for $\chi''(H_1)$ are presented in Fig. 2(c), with the model results in Fig. 2(d). The hysteresis found in $\tilde{\chi}(H_{dc})$ is shown more clearly in Fig. 2(e) for successive scans 1, 2, 3, . . . , for $0 \leq H_{dc} \leq 100$ Oe; a larger hysteresis is found in scans to 800 Oe, shown in Figs. 2(f) and 2(g).

Modified critical-state model. To understand the above rather complicated data we start with a two-dimensional model of Clem¹¹ for a long cylindrical sample of radius R containing long, superconducting "grains" of radius R_g and penetration depth λ_g , the remaining volume being assumed to be the so-called intergranular region of weak links, e.g., Josephson-junction barriers, with penetration depth λ_j ; we assume $R \gg R_g \gg \lambda_g$ and $\lambda_j \gg \lambda_g$, and an applied field $H_a(t, r = R) = H_{dc} + H_1 \cos(2\pi ft)$ parallel to the cylinder axis. After zero field cooling let the applied field be increased to some value $H_a > H_{c_{1j}}$, the lower critical field for the intergranular region; flux lines of B , in units of fluxons $hc/2e$, enter through the cylinder walls giving rise to self-induced circular shielding currents of density J , which pull the fluxons inward with a Lorentz force density¹² $F_L = |\mathbf{J} \times \mathbf{B}|/c \approx -(dH/dr)B/4\pi$, where $H(r)$ is the local magnetic field in the cylinder created by the shielding current $J(r)$; F_L is essentially the gradient of the magnetic pressure. The fluxons quickly move in until $|F_L| \leq \alpha_c$ at all points in the sample, where α_c is the fluxon pinning force density arising from lattice defects, impurities, etc., and is sample dependent. This state is called the critical state⁴⁻⁶ in which there is no net force on the fluxons and $J \rightarrow J_c$, the critical value of the current density, experimentally known to depend on the local field H . Except for slow thermally activated flux creep the critical state is a (barely) stable state and will be assumed to be maintained for sufficiently small and slow

changes in H_a . If H_a is now reduced, fluxons will be forced outward through the cylinder walls by a reversed shielding current density, leaving, however, some fluxons trapped in the sample. The above process is concisely stated by the critical-state equation of Bean:⁴

$$dH/dr = (\pm)4\pi J_c(H)/c \quad (1)$$

for the local field H , where (\pm) is determined by the sign of the electromotive force. The equation predicts the magnetization loop $M(H)$ vs H , with hysteresis, as observed in type-II superconductors. Equation (1), with a suitable equation for $J_c(H)$, allows a calculation of the local field $H(r)$; and with $H_a(t)$, the time-dependent local field $H(r,t)$ in the sample, and its spatial average value $\bar{H}(t)$.^{2,7-9,13} From $\bar{H}(t)$ we calculate the real and imaginary parts of $\tilde{\chi}$ (Gaussian units) defined by

$$1 + 4\pi\chi' = \frac{\omega}{\pi H_1} \mu_{\text{eff}} \int_0^{2\pi/\omega} \bar{H}(t) \cos(\omega t) dt, \quad (2)$$

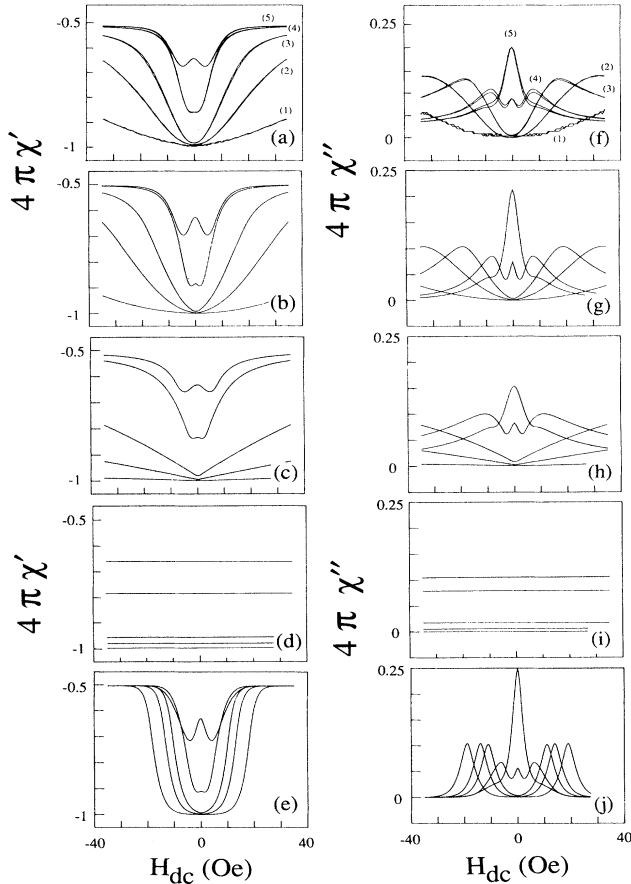


FIG. 1. (a) Measured ac susceptibility $\chi'(H_{\text{dc}})$ (Gaussian units) for a $\text{YBa}_2\text{Cu}_3\text{O}_7$ sample at $T=78.3$ K and $f=10$ kHz for values of ac field H_1 (Oe): (1) 0.03, (2) 0.22, (3) 0.71, (4) 4.03, (5) 7.91. (b) Modified critical-state model prediction for the data of (a) using parameters $\beta=2.25$ and $H_0=3.0$ Oe in Eq. (4). (c) Same as (b) but with $\beta=1.0$. (d) Same as (b) but with $\beta=0$. (e) Critical-state model prediction for exponential dependence of $J_c(H)$. (f)–(j) same as (a)–(e), but $\chi''(H_{\text{dc}})$ plotted.

$$4\pi\chi'' = \frac{\omega}{\pi H_1} \mu_{\text{eff}} \int_0^{2\pi/\omega} \bar{H}(t) \sin(\omega t) dt, \quad (3)$$

where μ_{eff} is a geometrical filling factor. These equations are used, with suitable parameters, to separately compute the contributions of the inter- and intragranular components to the total $\tilde{\chi} = \tilde{\chi}_J + \tilde{\chi}_g$. Here we report model predictions only for $\tilde{\chi}_J$, observed in the low-field region, $H_a \lesssim 50$ Oe.

The key to a good model of $\tilde{\chi}(H_{\text{dc}}, H_1)$ is a realistic expression for $J_c(H)$ based on experimental data rather than simple assumptions. In our modified critical-state model for the intergranular region we use

$$J_c(H) = \alpha' c / (|H| + H_0)^\beta \quad (4)$$

where α' is a fluxon pinning parameter, assumed field independent, and H_0 and β are parameters that determine the form of $J_c(H)$ and are to be determined by a fit to our data. The parameter α' is related to the fluxon pinning force density $\alpha_c = \alpha' / (|H| + H_0)^{\beta-1}$. Bean's simplified model assumed $\beta=0$; Anderson and Kim assumed $\beta=1$, as did Müller² and Ishida and Goldfarb³ in models and measurements of $\tilde{\chi}$ in $\text{YBa}_2\text{Cu}_3\text{O}_7$, finding good agreement for the temperature dependence.

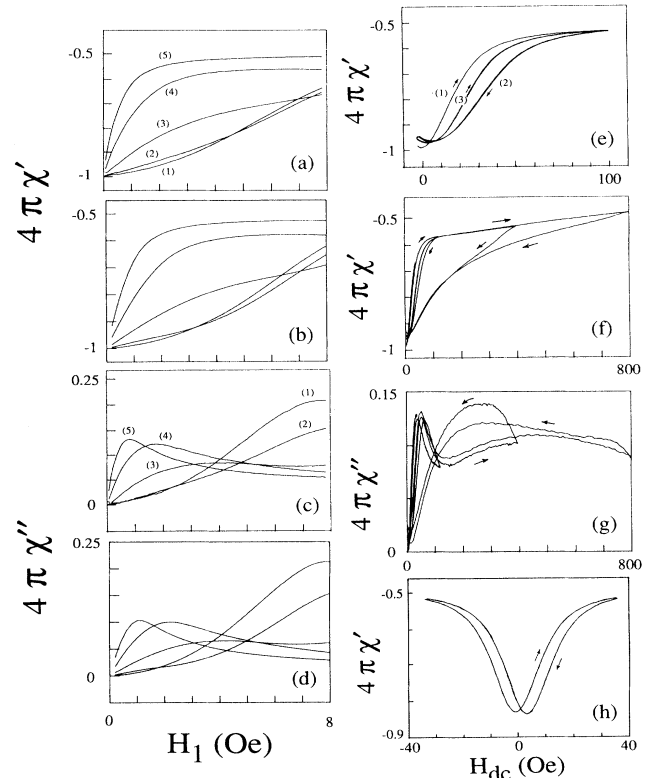


FIG. 2. (a) Measured ac susceptibility $\chi'(H_1)$ for a $\text{YBa}_2\text{Cu}_3\text{O}_7$ sample at $T=78.3$ K and $f=10$ KHz for values of dc field H_{dc} (Oe): (1) 0, (2) 2, (3) 5, (4) 10, (5) 15. (b) Modified critical-state model prediction for the data of (a) using parameters $\beta=2.25$ and $H_0=3.0$ Oe in Eq. (4). (c),(d) Same as (a),(b) but $\chi''(H_1)$ plotted. (e)–(h) measured hysteresis of ac susceptibility $\tilde{\chi}(H_{\text{dc}})$ at $H_1=0.22$ Oe, $T=78.3$ K.

We now discuss transport measurements of $J_c(H)$ for $\text{YBa}_2\text{Cu}_3\text{O}_7$ bars at $T=77$ K, particularly those of Ekin *et al.*,¹⁴ Peterson and Ekin,^{15,16} and Male *et al.*¹⁷ Although different samples have different maximum J_c , the dependence of $J_c(H)$ is somewhat invariant and may be described as follows in terms of three regions: (i) $J_c \approx 300$ A/cm² remains constant for $0.03 \lesssim H \lesssim 3$ Oe and then falls as $J_c \propto H^{-\gamma}$ with $1.5 \lesssim \gamma \lesssim 2$ to a (ii) plateau at $J_c \approx 10$ A/cm² in the region $100 \lesssim H \lesssim 3000$ Oe, where it again (iii) falls rapidly to $J_c \approx 0.1$ A/cm² as $H \rightarrow 10^5$ Oe. These regions are identified¹⁵ as follows. Region (i): Current limited by Josephson weak links or junctions with field dependence best described by an Airy diffraction pattern, averaged over a distribution of junction lengths and orientations¹⁶; this model is in good agreement with their transport $J_c(H)$ data and predicts a flat region at very low fields followed by a falloff, $J_c \propto (H/H_0)^{-3/2}$, where $H_0 = [(hc/2e)/\text{grain area}] \approx 3-5$ Oe. The data of Male *et al.*¹⁷ show similar behavior with $J_c \propto H^{-2}$ in the same region. Equation (4) can be seen to be a simple algebraic approximation for region (i). Region (ii): Current limited by remanent percolation paths in a small volume fraction of the sample. Region (iii): Flux flow region as $H \rightarrow H_{c2}$ for the weakest link. Except for Figs. 2(f) and 2(g), our data are taken in region (i), hence the form of Eq. (4), with the expectation that $\beta \approx 2$.

Model parameters. At some constant temperature the model [Eqs. (1)–(4)] predicts χ' and χ'' as functions of the experimentally known parameters (H_{dc}, H_1, R) and those characterizing sample properties (α', H_0, β , and μ_{eff}). However, there is an additional relationship $\alpha' = [(H^* + H_0)^{\beta+1} - H_0^{\beta+1}] / [4\pi(\beta+1)R]$, where H^* is the value of H_a for which the flux front just reaches $r=0$, corresponding to a maximum of $\chi''(H_1)$ at $H_1 = H^*$, readily measured⁸ to be ≈ 8.0 Oe. The saturated value $4\pi\chi' \rightarrow \mu_{\text{eff}} - 1$ for $H_a \gtrsim 20$ Oe, yielding $\mu_{\text{eff}} = 0.49$. Thus there are only two parameters, β and H_0 , to be fit by the experimental data $\tilde{\chi}(H_{dc}, H_1)$; from these one can find α' from the relationship $H^* = [4\pi\alpha'(1+\beta)R + H_0^{\beta+1}]^{1/(\beta+1)} - H_0$, derived by the model. The best fit to the $\tilde{\chi}$ data of Figs. 1(a) and 1(f) was found for the parameters $\beta=2.25$ and $H_0=3.0$ Oe, yielding the modified critical-state predictions shown in Figs. 1(b) and 1(g), which closely agree with data both as a function of H_{dc} and of H_1 . Those parameters correspond to a pinning parameter $\alpha' = 688$ Oe^{3.25}/cm and a pinning force density $\alpha_c = 174$ Oe²/cm. Similar data at $T=82.5$ K also showed good agreement with the model using $\beta=2.22$ and $H_0=2.5$ Oe. Data at $T=85.7$ K are well explained by the model with $\beta=2.20$ and $H_0=2.0$ Oe, except for the hysteresis.

Figures 1(c) and 1(h) show the predictions if β is changed to 1.0, and are seen to fail to fit at small H_1 . If we use $\beta=0$, the predictions as seen in Figs. 1(d) and 1(i) do not agree at all, since this assumes no field dependence of J_c . For an assumed exponential field dependence,¹⁸ $J_c(H) \propto \exp(-|H|/H_e)$, the best fit, obtained for $H_e \approx 2.5$ Oe, still fails noticeably at large H , as shown in Figs. 1(e) and 1(j). We conclude that detailed $\tilde{\chi}(H_{dc}, H_1)$ data are very sensitive to $J_c(H)$ and can in fact be used to determine $J_c(H)$.

Hysteresis of $\tilde{\chi}(H_{dc})$. The small hysteresis in Fig. 1(f) is revealed more fully in Fig. 2(h), in sample No. 2, from a different batch of $\text{YBa}_2\text{Cu}_3\text{O}_7$. The central feature is that $\chi'(H_{dc})$ for symmetric scanning between $\pm H_{dc}|_{\text{max}}$ shows two minima near $H_{dc}=0$, shifted to a higher (lower) field for field decreasing (increasing). Both χ' and χ'' have the property $\chi(H_{dc})|_{s=1} = \chi(-H_{dc})|_{s=-1}$, with $s = \text{sgn}(dH/dt)$. If $|H_{\text{max}}| \neq |H_{\text{min}}|$, this symmetry breaks down. The splitting ΔH between the minima is a measure of the hysteresis, and increases with increasing temperature and decreasing H_1 and is somewhat sample dependent. This behavior of $\tilde{\chi}$ has not been previously reported, to our knowledge, but appears to be related both to the coherent-detected second-harmonic voltage and to modulated microwave power absorption in $\text{YBa}_2\text{Cu}_3\text{O}_7$.¹⁹ Figures 2(f) and 2(g) with separate scans up to $H_{\text{max}} = 40, 100, 400,$ and 800 Oe show a clear distinction between the intergranular contribution to $\tilde{\chi}$ for $H_{dc} \lesssim 50$ Oe [with small hysteresis, weak pinning, saturation of $\chi'(H_{dc})$, and a peak in $\chi''(H_{dc})$ at ≈ 40 Oe] and the intragranular contribution for $H_{dc} \gtrsim 80$ Oe (with very large hysteresis, strong pinning, minimal structure of χ' , and a very broad peak in χ'' at ≈ 400 Oe). If the sample is powdered, the features below $H_{dc} \approx 50$ Oe disappear. We point out that this hysteresis in $\tilde{\chi}$ cannot be formally predicted by the above critical-state models for either component, owing to the assumption that the critical current density J_c depends only on the magnitude of the local field H , according to Eq. (4). Most transport measurements report $J_c(H)$ measured after zero field cooling and then monotonic increase in H . However, Male *et al.*¹⁷ report J_c for a well-characterized $\text{YBa}_2\text{Cu}_3\text{O}_7$ bar at 77 K for a perpendicular applied field, first increasing to a field H_{max} and then decreasing to zero (for $H_{\text{max}} = 100, 300,$ and 500 Oe), showing a hysteresis in $J_c(H_{dc})$ quite similar to $\chi'(H_{dc})$ in Fig. 2(f). The fact that J_c depends not only on H but also the magnetic history is a likely source of the hysteresis in Fig. 2(f), with strong intragranular pinning, as well as in Fig. 2(h), with much weaker intergranular pinning. Evetts and Glowacki²⁰ have proposed a mechanism for hysteresis in $J_c(H_{dc})$.

To summarize, for the $\text{YBa}_2\text{Cu}_3\text{O}_7$ at 78.3 K we report detailed data on $\tilde{\chi}$ as a function of small applied dc and ac fields, finding close agreement with a modified critical-state model assuming a critical current density $J_c(H) \sim H^{-2}$, a steeper field dependence than the original Bean, Anderson, Kim model, but in reasonable agreement with transport measurements. We find that $\tilde{\chi}(H_{dc})$ shows a small hysteresis for the intergranular component and much larger hysteresis for the intragranular component, neither being formally explicable by existing critical-state models, requiring further investigation.

This work was supported in part by the Director, Office of Energy Research, Office of Basic Energy Sciences, Materials Sciences Division of the U.S. Department of Energy under Contract No. DE-AC03-76SF00098, and by the Office of Naval Research under Contract No. N00014-86-K-0154.

- *Present address: Physics Department, Ajou University, 5 Wonchun-dong, Kwon Son-ku Suw On 441-749, Korea.
- ¹R. B. Goldfarb, A. F. Clark, A. I. Braginski, and A. J. Panson, *Cryogenics* **27**, 475 (1987); H. Mazaki *et al.*, *Jpn. J. Appl. Phys.* **26**, L1749 (1987); F. Gomory and P. Lobotka, *Solid State Commun.* **66**, 645 (1988); V. Calzona, M. R. Cimberle, C. Ferdeghini, M. Putti, and A. S. Siri, *Physica C* **157**, 425 (1989); D. X. Chen, R. B. Goldfarb, J. Nogues, and K. V. Rao, *J. Appl. Phys.* **63**, 980 (1988); H. Kupfer *et al.*, *Cryogenics* **28**, 650 (1988); B. Renker *et al.*, *Z. Phys. B* **67**, 1 (1987); E. M. Gyorgy, R. B. Van Dover, K. A. Jackson, L. F. Schneemeyer, and J. V. Wasczak, *Appl. Phys. Lett.* **55**, 283 (1989).
- ²K.-H. Müller, *Physica C* **159**, 717 (1989); K.-H. Müller, J. C. McFarlane, and R. Driver, *Physica C* **158**, 69 (1989).
- ³T. Ishida and R. B. Goldfarb, *Phys. Rev. B* **41**, 8937 (1990).
- ⁴C. P. Bean, *Phys. Rev. Lett.* **8**, 250 (1962); *Rev. Mod. Phys.* **36**, 31 (1964).
- ⁵H. London, *Phys. Lett.* **6**, 162 (1963).
- ⁶Y. B. Kim, C. F. Hempstead, and A. R. Strnad, *Phys. Rev.* **129**, 528 (1963); P. W. Anderson and Y. B. Kim, *Rev. Mod. Phys.* **36**, 39 (1964).
- ⁷Youngtae Kim and C. D. Jeffries, *Bull. Am. Phys. Soc.* **35**, 338 (1990).
- ⁸Youngtae Kim, Ph.D. thesis, 1990, University of California, Berkeley (unpublished).
- ⁹Q. H. Lam, Youngtae Kim, and C. D. Jeffries, *Phys. Rev. B* **42**, 4846 (1990).
- ¹⁰YBa₂Cu₃O₇ sample provided by National Superconductor Inc.; measured density $\rho \approx 4.1 \text{ g cm}^{-3}$; measured $T_c \approx 92 \text{ K}$.
- ¹¹J. R. Clem, *Physica C* **152-155**, 50 (1988).
- ¹²See, e.g., M. Tinkham, *Introduction to Superconductivity* (McGraw-Hill, New York, 1975), Secs. 5.4–5.7.
- ¹³L. Ji, R. H. Sohn, G. C. Spalding, C. J. Lobb, and M. Tinkham, *Phys. Rev. B* **40**, 10 936 (1989).
- ¹⁴J. W. Ekin, T. M. Larson, A. M. Herman, Z. Z. Sheng, K. Togano, and H. Kumakura, *Physica C* **160**, 489 (1988).
- ¹⁵R. L. Peterson and J. W. Ekin, *Phys. Rev. B* **37**, 9848 (1988).
- ¹⁶R. L. Peterson and J. W. Ekin, *Physica C* **157**, 325 (1989).
- ¹⁷S. E. Male, J. Chilton, A. D. Caplin, C. N. Guy, and S. B. Newcomb, *Supercond. Sci. Technol.* **2**, 9 (1989).
- ¹⁸G. Ravi Kumar and P. Chaddah, *Phys. Rev. B* **39**, 4704 (1989); P. Chaddah *et al.*, *Physica C* **159**, 570 (1989).
- ¹⁹C. D. Jeffries, Q. H. Lam, Y. Kim, C. M. Kim, A. Zettl, and M. P. Klein, *Phys. Rev. B* **39**, 11 526 (1989), Figs. 14 and 15.
- ²⁰J. E. Evetts and B. A. Glowacki, *Cryogenics* **28**, 641 (1988).